

## **Truncated least square support vector machine for parameter estimation of a nonlinear manoeuvring model based on PMM tests**

Haitong Xu<sup>a</sup>, Vahid Hassani<sup>b,c</sup>, C. Guedes Soares<sup>a\*</sup>

<sup>a</sup> *Centre for Marine Technology and Ocean Engineering (CENTEC), Instituto Superior Técnico, Universidade de Lisboa, Av. Rovisco Pais, 1049-001 Lisboa, Portugal.*

<sup>b</sup> *Department of Mechanical, Electronics and Chemical Engineering, Oslo Metropolitan University, Oslo, Norway*

<sup>c</sup> *Department of Ships and Ocean Structures, SINTEF Ocean, Trondheim, Norway*

*\*Corresponding author email: [c.guedes.soares@centec.tecnico.ulisboa.pt](mailto:c.guedes.soares@centec.tecnico.ulisboa.pt)*

### **ABSTRACT**

A new version of least square support vector machine (LS-SVM), the truncated LS-SVM, is proposed to estimate the nondimensionalized hydrodynamic coefficients. Truncated LS-SVM is shown to be an efficient and robust method that avoids the costly matrix inversion operation in classical LS-SVM using the singular values decomposition. Meanwhile, the smaller singular values are neglected considering their negligible contribution to the solutions. In order to get a robust parameter estimation, the model simplification of the nonlinear manoeuvring model is carried out using a leave-one-out method, considering the trade-off between the parameter uncertainty and accuracy of the numerical model. The simplified manoeuvring model and the values of nondimensionalized hydrodynamic coefficients are presented. The coefficients are estimated using Planar motion mechanism (PMM) tests, which were carried out in a towing tank. The validation process is carried to validate the generalization performance of the obtained numerical model using the PMM test data.

*Keywords:* Truncated support vector machine; Parameter estimation; Model reduction; Nonlinear Manoeuvring Model; Planar Motion Mechanism test.

## **NOMENCLATURE**

$u, v, w$	Velocity in surge, sway and heave
$U$	Ground speed
$\beta$	Drift angle
$\mathcal{S}$	Training set
$\mathbf{w}$	Weight matrix
$\varphi(x)$	Kernel function
$b$	Bias term
$C$	Regularization factor
$L(\mathbf{w}, b, e_i, \alpha_i)$	Lagrange function
$\sum_{i=1}^N e_i^2$	Empirical error
$A$	Kernel matrix
$Y$	Output matrix
$\theta$	Parameter matrix
$U$	Left-singular vectors
$V$	Right-singular vectors
$\Sigma$	Singular values matrix
$U_r$	Truncated left-singular vectors
$V_r$	Truncated right-singular vectors

$\Sigma_r$	Truncated singular values matrix
$\boldsymbol{\eta}$	Generalized position defined in the North-East-Down frame
$\mathbf{v}$	Velocity and yaw rate of rigid body, expressed in Body-fixed frame
$\mathbf{M}_{RB}$	Rigid-body mass matrix
$\mathbf{C}_{RB}$	Rigid-body Coriolis-centripetal matrix
$\mathbf{M}_A$	Added-mass matrix
$\mathbf{C}_A$	Added Coriolis-centripetal matrix
$D(\mathbf{v})$	Nonlinear damping matrix
$\boldsymbol{\tau}$	Forces and moment
$\rho$	Water density
$L$	Ship length
$X'_{uu}, X'_{uuu} \dots$	Surge nondimensionalized hydrodynamic coefficients
$Y'_{uv}, Y'_{uv}, \dots$	Sway nondimensionalized hydrodynamic coefficients
$N'_{uv}, N'_{uv}, \dots$	Yaw nondimensionalized hydrodynamic coefficients
$R^2$	The goodness of fit criterion
$y_i$	Measurement data
$\hat{y}(x, \theta^*)$	Estimate values
$\bar{y}$	Mean value of measurement data

## 1. Introduction

With the development of numerical computation, the simulations of manoeuvring ships are drawing more attention due to the requirements of ship operation and autopilot design. Vessel simulators [1,2], can be used to train the ship handler and test the autopilot in a

virtual environment (also well-known as Hardware-in-the-loop Testing [3,4]). It plays an important role for the complex marine control systems [5], where the controller can be tested and is tuned in the virtual environment or Hardware-in-the-loop testing system. Hardware-in-the-loop testing system or vessel simulator can significantly reduce costs of the controller design for complex systems. A mathematical manoeuvring model is important for the vessel simulator, because it describes the response of a ship moving at sea.

Many manoeuvring mathematical models have been proposed considering the specific application requirements. These models have different features and are proposed for different application purposes considering the trade-off between the complexity and fidelity. For example, Abkowitz model [6] is one of the most popular models. The hydrodynamic forces and moments are approximated using a 3-order truncated Taylor expansion techniques. Nomoto model [7], was proposed for autopilot design only considering the yaw motion. The MMG model was proposed considering the physical meaning of the forces and moment of the hull, propeller, and rudder, and the interaction effect between them [8,9]. The vectorial model is describing the motion of ships in a vectorial setting [10]. It benefits the designing of controllers and observers for ships and the stability analysis. The model of Sutulo and Guedes Soares, [11,12], allows the description of arbitrary 3DOF ship manoeuvring motions. A manoeuvring model considering the effect of shallow water and confined waterway can be found in [13–16].

Parameter estimation for manoeuvring models is an interesting and challenging topic [17]. The most reliable and effective method is to estimate the parameters based on Planar Motion Mechanism (PMM) tests of a scaled ship model. The PMM test usually can provide

rich information for parameter estimation [18]. It can isolate the effect due to the coupled motions, such as surge, sway and yaw. The tests need to be carried out in a towing tank, which usually indicate high cost and are time-consuming.

System identification is one of the promising methods to obtain the parameters from measured data [19]. Now it has been widely used for estimating the hydrodynamics coefficients for marine vehicles [19–26]. Many methods have been employed for parameter estimation, and the Least Squares (LS) is one of the most popular methods. Nonlinear viscous damping forces of a surface vessel were identified using the least squares method [19]. In [25], PMM tests, such as pure yaw, pure sway, mixed sway and yaw, were carried in a towing tank using scaled ship model. The hydrodynamic coefficients were identified using the collected data, such as forces, moments, velocity and acceleration of surge, sway and yaw motions. The obtained mathematical model was then validated by reproducing the zigzag manoeuvring test conducted in the full-scaled ship [27]. Sutulo and Guedes Soares, [20,28], proposed an optimal offline system identification method combining the least squares with genetic algorithm to estimate the nonlinear manoeuvring coefficients. Xu et al. [23], used an optimal system identification based on least squares method to estimate the hydrodynamic coefficients of a modified Abkowitz model using a free-running model test, and further similar studies can be found in [29].

The least squares method is a simple and popular method but has some disadvantages [17,30]. The least squares method is sensitive to the noise and produces non-consistent estimations [31]. The obtained parameters usually contain a large uncertainty and easily they can drift from the true values. In order to get a robust estimation, truncated singular value decomposition (TSVD) [32] was used to solve the ill-conditioned problem of the

least square method [33]. Truncated singular value decomposition neglects the smallest singular values [34]. Because the data corresponding to smaller singular values usually imposes more uncertainty in the process of estimating uncertain parameters. Söderström [30], used a regularized least-square method to solve the hyper-parameter estimation problem with large data sets and ill-conditioned computations. Tikhonov regularization [35] is a good option for solving the ill-posed problem. It can significantly improve the condition number by modifying the normal equations in the least squares method while leaving the estimated parameter relatively unchanged. The effect of Tikhonov regularization is to estimate the parameters while also keeping them near the reference values [36,37].

There are some other techniques used for the parameter estimation for ship manoeuvring. For example, in [26], the damping matrix of an underwater vehicle was estimated using neural networks. Perera et al. [38,39], used the Extended Kalman filter (EKF) to identify the parameters of a nonlinear vessel steering. The obtained steering model can be used to design the model-based heading controller. EKF was also used for observer design for underwater vehicles [40]. Maximum likelihood identification was used to design an adaptive wave filter for DP system [41]. In the last decade, a robust method, support vector machine (SVM), has been used for regression and parameter estimation [42]. SVM is a supervised machine learning algorithm, which can be used for both classification [43] or regression [44–46]. Xu and Guedes Soares [47,48], identified a nonlinear steering model for ship autopilot design using a least square support vector machine. Further studies can be found in [49–51]. Luo and Zou [21], used the least square support vector machine (LSSVM) to identify the hydrodynamic coefficients of an Abkowitz model. The further

work on this topic can be found in [22], in which, particle swarm optimization was employed to choose the regularization factor. Luo et al. [52] carried out manoeuvring simulation of a catamaran using support vector machines. Hou and Zou [53], identified the roll motion of floating structures in irregular waves using a  $\varepsilon$ -support vector regression. However, the obtained parameters using support vector machine also suffer the uncertainty problem due to noise. Both the linear and nonlinear hydrodynamic coefficients drift from the true value due to their large uncertainty. Multicollinearity is considered as the main reason for the parameter drift [22,54–56]. Multicollinearity is commonplace in the regression analysis, it is mostly due to the redundancy of the structure of the model [11]. Hwang [55], found the dynamic cancellation and the linear hydrodynamic coefficients drift simultaneously using slender-body theory. Luo and Li [54], used several methods, such as model simplification, parallel processing and additional excitation, to diminish the parameter drift. It needs to be pointed out that the main purpose of these methods is to reconstruct the samples and lighten the multicollinearity. The parameters with large uncertainty are sensitive to the noise and easily drift from the true values. So, it is necessary to analyze the parameter uncertainty induced by the noise. Xu et al. [50,56], used the singular value decomposition to give an explanation of the parameter uncertainty, Truncated singular value decomposition was used to diminish the parameter uncertainty and provide good results.

The main contribution of this paper is to propose a novel version of LS-SVM, i.e. the truncated least square support vector machine (TLS-SVM), and to employ it to estimate the nondimensionalized hydrodynamic coefficients. The proposed truncated LS-SVM is different from the method used by Wei et al. [57] and Zheng et al. [58], where singular

value decomposition (SVD) was employed for signal pre-processing, and the filtered data was then used for training the classical LS-SVM. The proposed truncated LS-SVM is trained by the singular value decomposition (SVD) of the kernel matrix. So, it can avoid the costly matrix inversion operation in classical LS-SVM. Meanwhile, the robust character can be achieved by ignoring the smaller singular values, because of their negligible contribution to the solutions.

The second contribution of this paper is to give a mathematical explanation for the parameter drift using singular value decomposition. Model reduction is carried out based on truncated LS-SVM. The PMM test data is used to identify the values of the hydrodynamic coefficients using truncated LS-SVM. Model reduction or model simplification was carried out based on leave-one-out method. The resulting models were further tested against the test training set. Most of them are not used in the training process. The  $R^2$  is used to demonstrate the accuracy of the obtained models. The results show that the simplified model works well and the truncated LS-SVM can provide a stable result and diminish the parameter uncertainty successfully.

The rest of the paper is organized as follows. Section 2 describes the planar motion mechanism (PMM) Tests. In section 3, the Truncated LS-SVM is introduced in detail and the uncertainty analysis of the identified parameters is given using singular value decomposition. A nonlinear manoeuvring model is briefly introduced in Section 4, and the multi-step parameter estimation and model simplification is carried out in Section 5. In section 6, Validation of the simplified nonlinear manoeuvring model is carried out. The final section is the conclusion.



## 2. Planar Motion Mechanism Tests

Scaled ship model tests are always the first choice when studying ship performance, because full-scale ship tests usually cost much money and time, although some information cannot be measured directly, such as forces acting on the rigid hull due to environmental disturbances. Computational fluid dynamics (CFD) is a very efficient tool for the study on manoeuvring of ships. It can provide rich information when ship moving in the sea, but the verification and validation of this method still have some way to go.

This section summarizes the series of PMM tests recommended by ITTC [18], such as pure yaw and pure sway. They were carried out using a scaled ship model in the tank of SINTEF Ocean, as presented in Fig. 1. The PMM test is commonly used for modelling the ship motions as it can provide rich information for system identification and get a reliable estimation of the parameters. Here, different PMM tests are introduced briefly. As presented in Fig.1, the ship model was fixed on a 6-DOF hexapod motion platform. The ship can move freely in 6 DOF. During the tests, the platform can control the ship moving as required by the tests. The forces and moment acting on the ship hull can be measured directly.

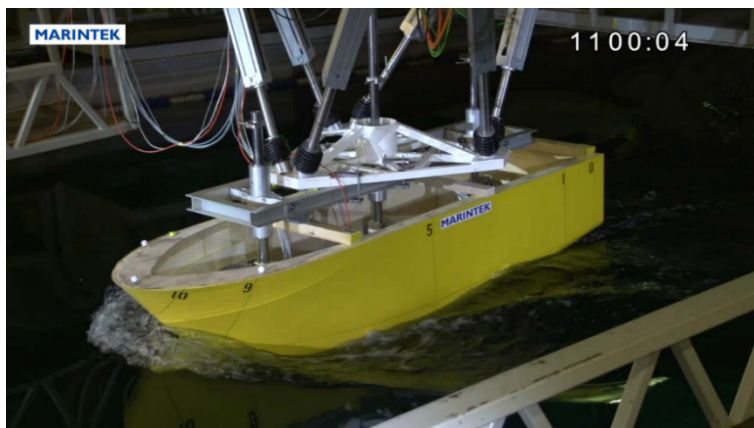


Fig. 1. PMM tests in a towing tank.

In pure surge test, the carriage tows the model forward with oscillations around a fixed surge speed. They are usually sinusoidal oscillations. During the tests, the sway speed and yaw rate are kept as zero ( $v=0$  and  $r=0$ ). So, the effect of sway and yaw can be eliminated from the surge motion model. This test aims to achieve the full response of surge motion. The trajectory of the pure surge is presented in Fig. 2(a).

In the pure drift test, the ship model is towed in a tank forward with a fixed drift angle  $\beta$ , as presented in Fig. 2(b). During the test, the surge and sway velocity is a non-zero constant, while the yaw rate is zero ( $u = U \cos(\beta), v = U \sin(\beta), r = 0$ ). So, the hydrodynamic coefficients related to the yaw motion can be neglected.

In a pure sway test, the carriage tows the model forward with oscillations around a fixed sway speed. This test can isolate the sway dynamics from the yaw motion. The surge speed of the ship is constant, and sway speed is sine wave ( $u = u_c, v = v_{\max} \cos(\omega t)$  and  $\psi = 0$ ). As presented in Fig. 2(c). The hydrodynamic coefficients related to the yaw motion can be neglected during the identification process.

In order to get the full response of yaw motion, the pure yaw test is a good choice. It can isolate the sway dynamics from the yaw motion. During the test, the output of the ship's yaw angle is a sine wave, meanwhile the surge speed is constant ( $u = u_c, v = 0$  and  $\psi = \psi_{\max} \sin(\omega t)$ ), as presented in Fig. 2(d).

Mixed sway and drift was carried out using a ship model with a sinusoidal oscillation in sway motion and a constant drift angle. The pathline is presented in Fig. 2(e). This test can provide the dynamic information of surge, sway and yaw motion. So, it can be used to estimate the coefficients related to the surge, sway and yaw motion. During the test, the

ground speed and drift angle is kept as constant, and yaw rate is set as a sinusoidal oscillation,  $U = U_c$ ,  $\beta = \beta_c$  and  $\psi = \psi_{\max} \sin(\omega t)$

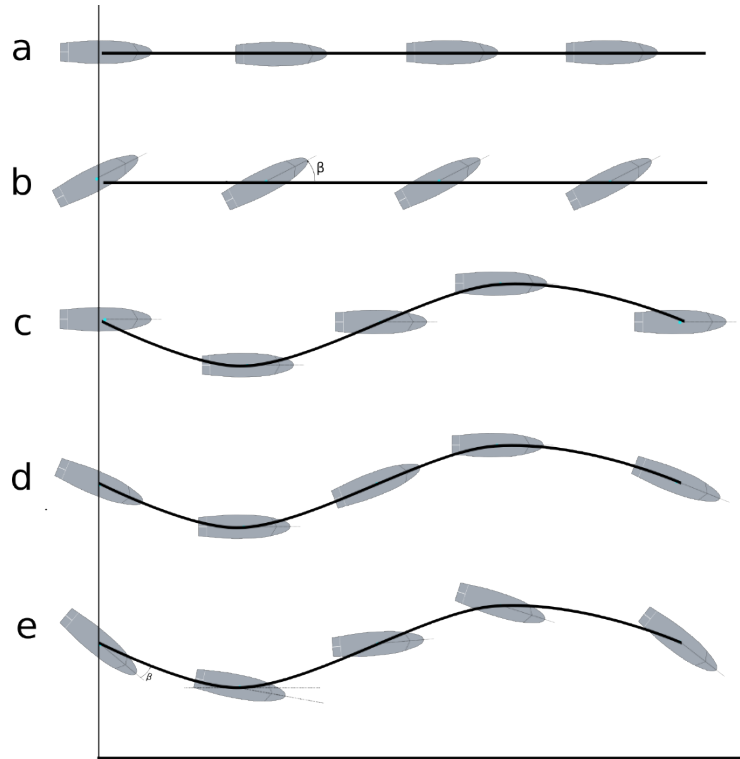


Figure 2. PMM test of ship model travelling along the pathline: (a) straight line (pure surge or surge acceleration); (b) pure drift; (c) pure sway; (d) pure yaw; (e) pure yaw +drift

### 3. Truncated least square support vector machine

The support vector machine, which was proposed by Vapnik [44], is a supervised machine learning algorithm widely used for both classification and regression [59]. Least square support vector machine (LS-SVM) proposed by Suykens and Vandewalle [43], is a modified version of SVM. By including the regularized squared error term in the SVM, the

solutions can be obtained by solving a set of linear equations instead of convex quadratic programming (QP) problem for classical SVMs. In this section, the classical LS-SVM will be introduced briefly. Then the truncated LS-SVM is proposed using singular value decomposition technology. Truncated LS-SVM is trained through the singular value decomposition (SVD) of the kernel matrix. So, it can avoid the matrix inversion operation, which is usually computationally expensive. Meanwhile, the truncated LS-SVM also neglect the effect of the small singular values and can provide a robust estimation.

### 3.1 Classical Least square support vector machine

Assume that there are  $N$  samples in the training set,  $\mathcal{S} = \{s_i | s_i = (x_i, y_i), x_i \in \mathfrak{R}^n, y_i \in \mathfrak{R}\}_{i=1}^N$ , where  $x_i$  is the input.  $y_i$  is the output. a general approximation function for regression purposes is:

$$y(x) = \mathbf{w}^T \boldsymbol{\varphi}(x) + b \quad (1)$$

where,  $x$  represents the training samples.  $y(x)$  are the target values.  $b$  is the bias term.  $\mathbf{w}$  is a weight matrix.  $\boldsymbol{\varphi}(x)$  is kernel function. Then, an optimization is formulated:

$$\begin{aligned} \min_{\mathbf{w}, b, e_i} \quad & f(\mathbf{w}, e) = \frac{1}{2} \mathbf{w}^T \mathbf{w} + \frac{1}{2} C \sum_{i=1}^N e_i^2 \quad (2) \\ \text{s.t.} \quad & y_i = \mathbf{w}^T \boldsymbol{\varphi}(x_i) + b + e_i \end{aligned}$$

where  $e_i, i = 1 \cdots N$ , is the error.  $C$  is the regularization factor. There is a trade-off between the model accuracy and the model complexity (also well-known as structural risk [59]). In order to solve Eq. (2), the Lagrange function is introduced. It is given as:

$$L(\mathbf{w}, b, e_i, \alpha_i) = \frac{1}{2} \mathbf{w}^T \mathbf{w} + \frac{1}{2} C \sum_{i=1}^N e_i^2 - \sum_{i=1}^N \alpha_i [\mathbf{w}^T \boldsymbol{\varphi}(x_i) + b + e_i - y_i] \quad (3)$$

where  $\alpha_i$  are the Lagrange multipliers. The Karush-Kuhn-Tucker conditions (KKT) [59], are defined by computing the derivative of Eq. (3) with respect to  $\mathbf{w}, b, e_i, \alpha_i$  :

$$\begin{aligned} \frac{\partial L}{\partial \mathbf{w}} = 0 &\rightarrow \mathbf{w} = \sum_{i=1}^N \alpha_i \boldsymbol{\varphi}(x_i) \\ \frac{\partial L}{\partial b} = 0 &\rightarrow \sum_{i=1}^N \alpha_i = 0 \\ \frac{\partial L}{\partial e_i} = 0 &\rightarrow \alpha_i = C e_i \\ \frac{\partial L}{\partial \alpha_i} = 0 &\rightarrow \mathbf{w}^T \boldsymbol{\varphi}(x_i) + b + e_i - y_i = 0 \end{aligned} \quad (4)$$

where  $i=1 \dots N$ . Rewriting Eq.4 in matrix representation.

$$\underbrace{\begin{bmatrix} 0 & \bar{\mathbf{1}} \\ \bar{\mathbf{1}} & K(\cdot) + C^{-1} \mathbf{I} \end{bmatrix}}_{\mathbf{A}} \underbrace{\begin{bmatrix} b \\ \bar{\boldsymbol{\alpha}} \end{bmatrix}}_{\boldsymbol{\theta}} = \underbrace{\begin{bmatrix} 0 \\ \bar{\mathbf{Y}} \end{bmatrix}}_{\mathbf{Y}} \quad (5)$$

where  $\mathbf{I}$  is an  $N \times N$  identity matrix.  $\bar{\boldsymbol{\alpha}} = [\alpha_1, \dots, \alpha_N]^T$ ,  $\bar{\mathbf{Y}} = [y_1, \dots, y_N]^T$ .  $K(x_k \cdot x_i) = \boldsymbol{\varphi}(x_k)^T \boldsymbol{\varphi}(x_i)$ ,  $i=1, \dots, N$  is the kernel function, which is an inner product between its operands. It is positive definite and satisfies the Mercer condition [43,44]. As presented in Eq. (5), the dimension of the matrix,  $\mathbf{A}$ , is  $(N+1) \times (N+1)$ . It is proportional to the length of the training set. So, if the training set is large, the classical LS-SVM fails to invert the matrix due to the heavy computation. Substitute  $\mathbf{w}$  in Eq. (1) with Eq. (4) and the kernel function ( $K(x_k \cdot x_i) = \boldsymbol{\varphi}(x_k)^T \boldsymbol{\varphi}(x_i)$ ), the LS-SVM model for the regression yields:

$$y(x) = \sum_{i=1}^N \alpha_i \boldsymbol{\varphi}(x_i)^T \boldsymbol{\varphi}(x) + b = \sum_{i=1}^N \alpha_i K(x \cdot x_i) + b \quad (6)$$

### 3.2 Truncated least square support vector machine

As presented in [21,54,55], the parameters drift from the true values when estimating the hydrodynamic coefficients using the least square support vector machine. Several methods for reconstructing the training data were used to diminish the parameter drift. In this section, the reason for the parameter drift is discussed using singular value decomposition. Then, a truncated least square support vector machine is proposed for the parameter estimations. Using singular value decomposition, the matrix,  $A$ , can be rewritten as

$$A = \sum_{i=1}^n u_i \sigma_i v_i^T = U \Sigma V^T \quad (7)$$

Then, the Eq. (5) can be rewritten as:

$$\theta = (U \Sigma V^T)^{-1} Y = V \Sigma^{-1} U^T Y = \sum_{i=1}^n \frac{v_i u_i^T}{\sigma_i} Y \quad (8)$$

where the matrix  $U$  and  $V$  are orthonormal,  $U^T U = I$  and  $V^T V = I$ .  $\Sigma$  is the diagonal matrix of the singular values of the matrix  $A$ .

Assume that there is an additive perturbation,  $\delta Y$ , it will propagate to a perturbation in the solution,

$$\delta \theta = V \Sigma^{-1} U^T \delta Y = \sum_{i=1}^n \frac{v_i u_i^T}{\sigma_i} \delta Y \quad (9)$$

As presented in Eq. (9), when the singular value,  $\sigma_i$ , is very small or close to the numerical precision of the computation, then the perturbation in the  $y$  is magnified and can potentially dominate the solutions,  $\theta_i$ . The corresponding columns of  $U$  and  $V$  contribute negligibly to the matrix  $A$ . Their contribution to the solution can be easily dominated by the noise

and round-off error in  $y$ . So, the corresponding parameters are easily affected by the noise in the data and drift from the true values with a large probability.

In order to get a physically meaningful solution, smaller singular values should be neglected or damped. Truncated singular value decomposition (TSVD) can be used to obtain a relatively accurate representation of the matrix  $A$ , by retaining the first  $r$  singular values of  $A$  and the corresponding columns of  $U$  and  $V$ . The TSVD can be presented as

$$A_r = U_r \Sigma_r V_r^T \quad (10)$$

where the matrix  $\Sigma_r$  is obtained by retaining the first  $r$  singular values of  $\Sigma$ . Similarly, matrices  $U_r$  and  $V_r$  are found using the corresponding singular vectors. The resulting  $A_r$  represents the reduced data set where the data related to the omitted singular values are filtered. The optimal value of  $r$  can be estimated using the *L-curve*, which is a log-log plot of the norm of a regularized solution versus the norm of the corresponding residual norm [35,36,60]. The flowchart of optimal Truncated LS-SVM is given in Fig. 3.

The covariance matrix of the parameter estimates,  $V_{\hat{\theta}}$ , was estimated using

$$V_{\hat{\theta}} = \left[ \frac{\partial \hat{\theta}}{\partial y} \right] V_y \left[ \frac{\partial \hat{\theta}}{\partial y} \right]^T = [X^T V_y^{-1} X]^{-1} \quad (11)$$

The covariance matrix is sometimes called the error propagation matrix, as it indicates how random measurement errors in the data  $y$ , as described by  $V_y$ , propagate to the model coefficients  $\hat{\theta}$ . The error of the parameters,  $\sigma_{\hat{\theta}}$  is the square-root of the diagonal of the parameter covariance matrix.

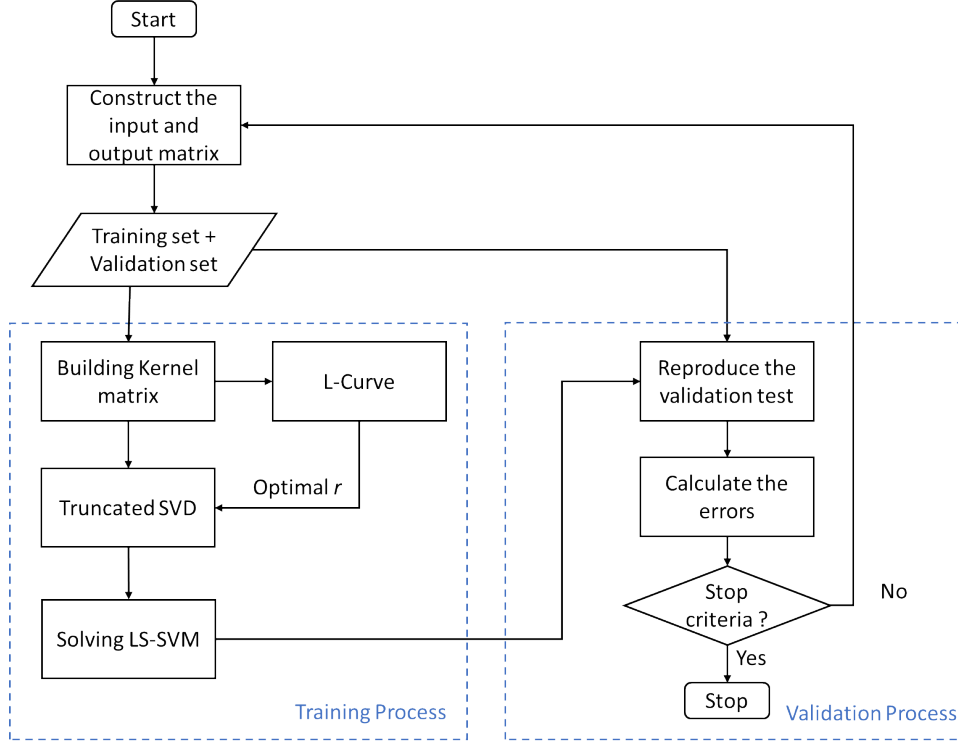


Figure 3: Flowchart of Optimal Truncated LS-SVM

#### 4. Nonlinear manoeuvring mathematical model

In this section, a nonlinear manoeuvring model in 3 degree of freedom (DOFs) is considered. This model was derived using the Kirchhoff-Motion-Equations [10,61,62]. The mathematical model for a marine surface vessel in 3-DOF (surge, sway and yaw) can be expressed as [10]:

$$\dot{\boldsymbol{\eta}} = \mathbf{R}(\boldsymbol{\psi})\mathbf{v} \quad (12)$$

$$\mathbf{M}_{RB}\dot{\mathbf{v}} + \mathbf{C}_{RB}(\mathbf{v})\mathbf{v} + \mathbf{M}_A\dot{\boldsymbol{\psi}} + \mathbf{C}_A(\boldsymbol{\psi})\boldsymbol{\psi} + \mathbf{D}(\mathbf{v})\mathbf{v} = \boldsymbol{\tau}_{prop} + \boldsymbol{\tau}_{rudder} + \boldsymbol{\tau}_{wind} + \boldsymbol{\tau}_{wave} + \boldsymbol{\tau}_{ext}.$$

where,  $\boldsymbol{\eta} = [N, E, \boldsymbol{\psi}]^T$  is the generalized position defined in the *North-East-Down* (NED).

$\mathbf{v} = [u, v, r]^T$  is the velocity and yaw rate in the body-fixed frame.  $\mathbf{M}_{RB}$  and  $\mathbf{M}_A$  are the mass matrix and added mass matrix.  $\mathbf{C}_{RB}(\mathbf{v})$  and  $\mathbf{C}_A(\boldsymbol{\psi})$  are the Coriolis-centripetal matrix



of the rigid-body and hydrodynamic Coriolis-centripetal matrix, respectively.  $\mathbf{D}(\mathbf{v})$  is the hydrodynamic damping matrix.  $\mathbf{R}(\psi)$  is the rotation matrix achieving transformation of linear velocity from BODY to NED. The mass matrix and Coriolis-centripetal matrix of the rigid-body,  $\mathbf{C}_{RB}(\mathbf{v})$ , is given:

$$\mathbf{M} = \begin{bmatrix} m & 0 & 0 \\ 0 & m & 0 \\ 0 & 0 & I_z \end{bmatrix} \quad (13)$$

$$\mathbf{C}_{RB} = \begin{bmatrix} 0 & 0 & -mv \\ 0 & 0 & mu \\ mv & -mu & 0 \end{bmatrix} \quad (14)$$

Added-mass matrix and hydrodynamic Coriolis-centripetal matrix,  $\mathbf{C}_A(\mathbf{v})$ , are given as in [10]:

$$\mathbf{M}_A = \begin{bmatrix} X_u & 0 & 0 \\ 0 & Y_v & Y_r \\ 0 & N_v & N_r \end{bmatrix} \quad (15)$$

$$\mathbf{C}_A(\mathbf{v}) = \begin{bmatrix} 0 & 0 & Y_v v + Y_r r \\ 0 & 0 & -X_u u \\ -Y_v v - Y_r r & X_u u & 0 \end{bmatrix} \quad (16)$$

Hydrodynamic damping forces are very complex and mainly caused by lift and drag, cross-flow drag, and vortex shedding [10]. They are the most awkward and ill-defined forces and moments acting on a ship. Here, the structure of nonlinear damping forces is adopted from [61,63], where the total damping forces are derived into two terms, damping due to lift and drag and crossflow drag. The total damping matrix is given:

$$D(\mathbf{v}) = \begin{bmatrix} -X_{uu}u - X_{uu}u^2 & -X_{vv}v - X_{rv}r & -X_{rr}r - X_{ur}ur \\ -X_{uv}vr - X_{u|v}|v| & -X_{uv}uv & \\ 0 & -Y_{uv}u - Y_{uv}u^2 - Y_{vv}v^2 & -Y_{ur}u - Y_{ur}u^2 - Y_{rr}r^2 \\ & -Y_{rv}r^2 - Y_{|v}|v| - Y_{|v}|r| & -Y_{vr}v^2 - Y_{|v}|v| - Y_{|r}|r| \\ 0 & -N_{uv}u - N_{uv}u^2 - N_{vv}v^2 & -N_{ur}u - N_{ur}u^2 - N_{rr}r^2 \\ & -N_{rv}r^2 - N_{|v}|v| - N_{|v}|r| & -N_{vr}v^2 - N_{|v}|v| - N_{|r}|r| \end{bmatrix} \quad (17)$$

During the captive model tests, the measured forces in the 3DOF nonlinear manoeuvring model described in Eq. (11) can be written as:

$$\boldsymbol{\tau}_{RB} = \mathbf{M}_A \dot{\mathbf{v}} + \mathbf{C}_A(\mathbf{v})\mathbf{v} + \mathbf{D}(\mathbf{v})\mathbf{v} \quad (18)$$

The equations of the hydrodynamic forces and moment can be expressed as follow:

$$\begin{aligned} X &= X_{\dot{u}}\dot{u} + Y_{\dot{v}}\dot{v} + Y_{\dot{r}}\dot{r} + X_{uu}uu + X_{uuu}uuu \\ &+ X_{rvu}rvu + X_{vv}vv + X_{rv}rv + X_{uvv}uvv + X_{rr}rr \\ &+ X_{urr}urr + X_{u|v}|u|v| \end{aligned} \quad (19)$$

$$\begin{aligned} Y &= Y_{\dot{v}}\dot{v} + Y_{\dot{r}}\dot{r} + X_{\dot{u}}ur + Y_{uv}uv + Y_{ur}ur + Y_{uur}uur \\ &+ Y_{uvv}uvv + Y_{vv}vvv + Y_{rr}rrr + Y_{rvv}rvv + Y_{vvr}vvr \\ &+ Y_{|v}|v|r| + Y_{|v}|v|v| + Y_{|r}|r|v| + Y_{|r}|r|r| \end{aligned} \quad (20)$$

$$\begin{aligned} N &= N_{\dot{v}}\dot{v} + N_{\dot{r}}\dot{r} + (Y_{\dot{v}} - X_{\dot{u}})vu + Y_{\dot{r}}ur \\ &+ N_{uv}uv + N_{ur}ur + N_{uur}uur + N_{uvv}uvv + N_{vv}vvv \\ &+ N_{rr}rrr + N_{rvv}rvv + N_{vvr}vvr + N_{|r}|r|v| \\ &+ N_{|v}|v|v| + N_{|r}|r|v| + N_{|r}|r|r| \end{aligned} \quad (21)$$

Obviously, these damping forces are too complex, and there are some redundant terms that produce similar effects, such as  $N_{|v}|v|r|$  and  $N_{rvv}rvv$ ,  $N_{rr}rrr$  and  $N_{|r}|r|r|$ . This almost certainly would result in overfitting and multicollinearity [11], which is also confirmed in reference [56]. So, it is necessary to simplify the above models.

## 5. Parameter estimation and simplification of the Nonlinear Manoeuvring model

In this section, the regression analysis will be carried out based on PMM tests, which were introduced in section 2. The effect of each similar term in the damping matrix will be analysed using a leave-one-out method. The main idea is to neglect the hydrodynamic coefficients with the largest uncertainty, then check if the new model still can reproduce the experimental results with good accuracy. In order to simplify the problem, multi-step system identification method based on truncated LS-SVM will be employed during the regression analysis. The  $R^2$  is used to measure the goodness of the fitness, as given in Eq. (22). If  $R^2$  is close to 1, it indicates that the obtained mathematical model can fully explain the test data.

$$R^2 = 1 - \frac{\sum [y_i - \hat{y}(x; \theta^*)]^2}{\sum [y_i - \bar{y}]^2} \quad (22)$$

In order to compare the coefficients of different ships and to estimate the dynamics of a full-size ship, the hydrodynamic parameters need to be converted to dimensionless ones. The prime system of SNAME (1950) will be used to normalize the hydrodynamic coefficients. The water density,  $\rho$ , the ship length  $L$  and the shipping speed  $U$  are employed as characteristic dimensional parameters. The list of the non-dimensionalisation factors and corresponding coefficients in Eqs. (19-21) is shown in Table 1.

Table 1. Dimensional factors for nondimensionalising the hydrodynamic coefficients.

Coef.	Dimensional Factor	Coef.	Dimensional Factor	Coef.	Dimensional Factor
$X'_u$	$0.5\rho L^3$	$Y'_v$	$0.5\rho L^3$	$N'_v$	$0.5\rho L^4$
$X'_u$	$0.5\rho L^2 U$	$Y'_r$	$0.5\rho L^4$	$N'_r$	$0.5\rho L^5$
$X'_{uu}$	$0.5\rho L^2$	$Y'_{uv}$	$0.5\rho L^2$	$N'_{uv}$	$0.5\rho L^3$

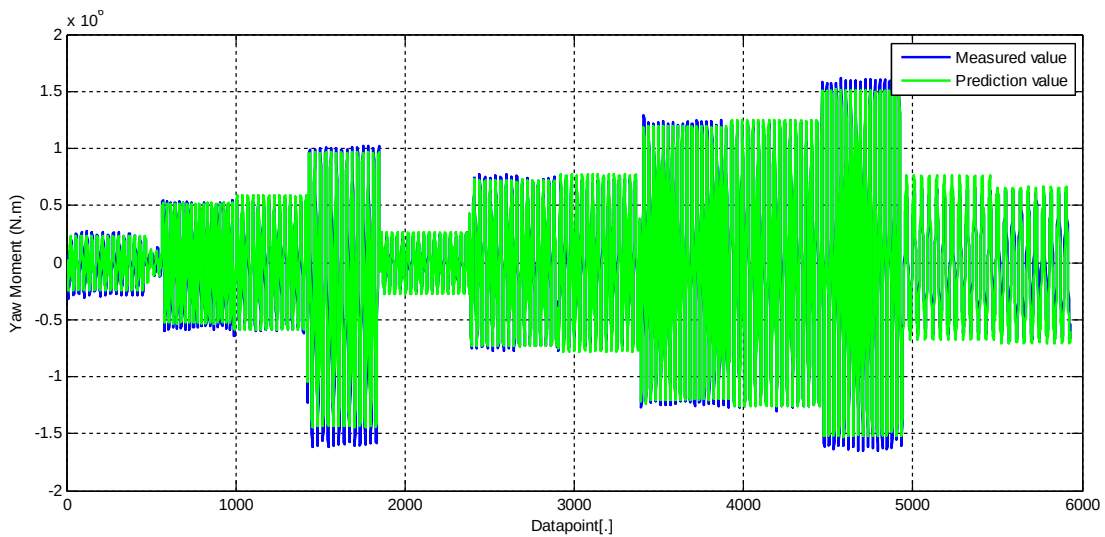
$X'_{uuu}$	$0.5\rho L^2 U^{-1}$	$Y'_{ur}$	$0.5\rho L^3$	$N'_{ur}$	$0.5\rho L^4$
$X'_{rvu}$	$0.5\rho L^3 U^{-1}$	$Y'_{uur}$	$0.5\rho L^3 U^{-1}$	$N'_{uur}$	$0.5\rho L^4 U^{-1}$
$X'_{vv}$	$0.5\rho L^2$	$Y'_{uuv}$	$0.5\rho L^2 U^{-1}$	$N'_{uuv}$	$0.5\rho L^3 U^{-1}$
$X'_{rv}$	$0.5\rho L^3$	$Y'_{vv}$	$0.5\rho L^2 U^{-1}$	$N'_{vv}$	$0.5\rho L^3 U^{-1}$
$X'_{uvv}$	$0.5\rho L^2 U^{-1}$	$Y'_{rr}$	$0.5\rho L^5 U^{-1}$	$N'_{rr}$	$0.5\rho L^6 U^{-1}$
$X'_{rr}$	$0.5\rho L^4$	$Y'_{rv}$	$0.5\rho L^4 U^{-1}$	$N'_{rv}$	$0.5\rho L^5 U^{-1}$
$X'_{urr}$	$0.5\rho L^4 U^{-1}$	$Y'_{vvr}$	$0.5\rho L^3 U^{-1}$	$N'_{vvr}$	$0.5\rho L^3 U^{-1}$
$X'_{u v }$	$0.5\rho L^2$	$Y'_{v v }$	$0.5\rho L^3$	$N'_{v v }$	$0.5\rho L^4$
		$Y'_{v v }$	$0.5\rho L^2$	$N'_{v v }$	$0.5\rho L^3$
		$Y'_{r v }$	$0.5\rho L^3$	$N'_{r v }$	$0.5\rho L^4$
		$Y'_{r r }$	$0.5\rho L^4$	$N'_{r r }$	$0.5\rho L^5$

The classical LS-SVM have a poor generalization performance when the training set is large scale. As suggested by Suykens [59], the size of the training set should be less than 2000. Before employing the proposed truncated LS-SVM for the parameter estimation, the classical LS-SVM is used to estimate the parameter of yaw motion. The obtained numerical model is then validated with the test set. The yaw model, as illustrated in Eq. (41), was chosen. The length of the training set is 6000, which is greater than the suggested number [59]. The LS-SVM toolbox [59] is chosen for approaching the yaw model. The training process is carried out and the numerical prediction is compared with the experimental data, as presented in Fig. 4 (a). The obtained model approximates the yaw moment in the training set successfully. The  $R^2$  is 0.9938 and the errors are zero as presented in Table 2. It indicates that the obtained model can fully explain the training set. However, the validation process is carried out and the result is presented in Fig. 4 (b), which shows that the obtained numerical yaw model has a poor generalization performance and failed to reproduce the yaw moment in the validation set. The  $R^2$  is  $-9.24E+19$ , it indicated the obtained model failed to predict the yam moments. Therefore,

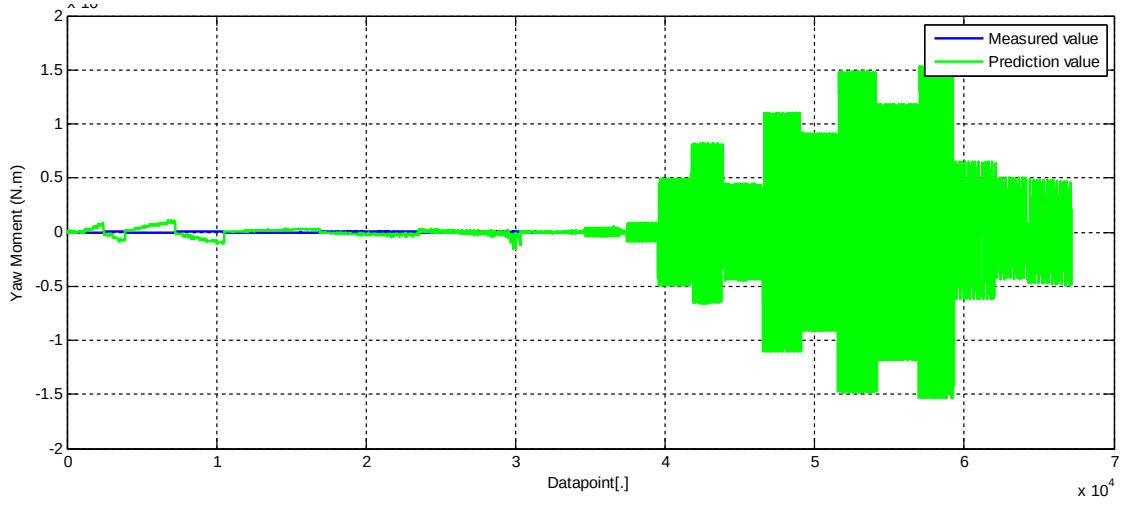
in order to obtain a robust parameter estimation, the optimal truncated LS-SVM will be used in the following part. The result shows that the truncated LS-SVM works with a large training set and provide a robust parameter estimation.

Table 2. Values of the hydrodynamic coefficient of yaw motion using classical LS-SVM and Truncated LS-SVM

Coef.	Truncated LS-SVM		LS-SVM	
	Value	Error (%)	Value	Error (%)
$N'_\dot{r}$	-1.20E-03	0.19	-3.78E+07	0
$N'_\dot{\psi}$	1.87E-03	0.65	-3.67E+07	0
$N'_{uur}$	-8.41E-03	0.20	-1.91E+06	0
$N'_{r r }$	-1.00E-03	2.50	2.14E+06	0
$N'_{uv}$	2.14E-02	0.10	1.28E+07	0
$N'_{v r }$	-1.69E-02	0.40	-7.35E+05	0
$N'_{r v }$	1.11E-02	0.73	4.03E+05	0



(a)



(b)

Figure 4. The modelling the yaw motion using the classical LS-SVM, (a: training process; b: validation process).

### 5.1 Regression analysis of surge motion

First, pure surge and pure sway will be used for training purposes. The surge model can be simplified due to the zero-yaw. It can be rewritten as:

$$X' = X'_{\dot{u}} \dot{u}' + X'_{uu} u' u' + X'_{uuu} u' u' u' + X'_{vv} v' v' + X'_{uvv} u' v' v' + X'_{u|v|} u' |v'| \quad (23)$$

The nondimensionalized parameters and corresponding deviations are presented in table 2. From the table, the term,  $X'_{vv}$ , failed to be estimated due to the large deviation. The terms,  $X'_{uuu}$  and  $X'_{uu}$ , are with the same values and different sign. The terms,  $X'_{uvv}$  and  $X'_{u|v|}$ , also produce similar effects. so, a new revised model can be proposed as:

$$X' = X'_u \dot{u}' + X'_{uuu} u' u' u' + X'_{uvv} u' v' v' \quad (24)$$

The values for the new model is given in Table 3. Obviously, the new model is more stable and simple compared with the previous one. The  $R^2$  values for both models are 0.754 and 0.753, respectively. So, the revised model can also agree with the training data well.

Table 3. The values of the parameters and their deviations for the surge models using pure surge and pure sway test data.

Coef.	Old model Eq.(23)		Revised model Eq.(24)	
	Value	Error (%)	Value	Error (%)
$X'_u$	-1.11E-02	0.64	-1.11E-02	0.65
$X'_{uu}$	1.02E+00	14.91	-	-
$X'_{uuu}$	-1.02E+00	14.90	-7.25E-05	7.23
$X'_{vv}$	1.42E-02	53.69	-	-
$X'_{uvv}$	-5.63E-01	14.15	-4.69E-02	1.60
$X'_{u v }$	-9.82E-04	31.49	-	-

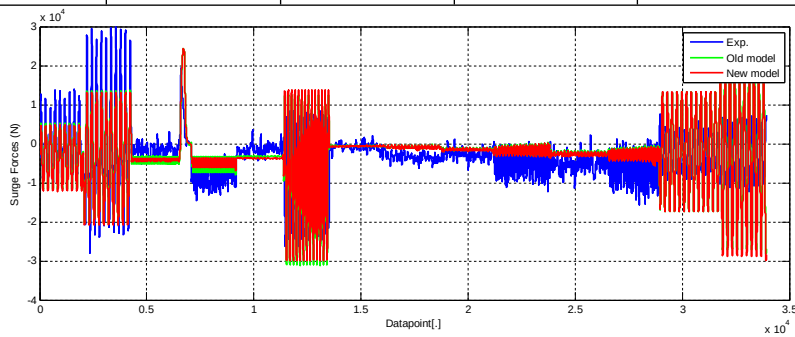


Figure 5: The pure surge and pure sway test reproduced based on the obtained surge models.

The surge forces are reproduced using both models, and the result is presented in Fig. 5. Then, a training set contains pure surge, pure sway and pure yaw is used to analyse the surge motion. considering the previous discussion, the new surge model can be written as:

$$X' = X'_u \dot{u}' + Y'_v v'r' + Y'_r r'r' + X'_{uuu} u'u'u' + X'_{uvv} u'v'v' + X'_{rvu} r'v'u' + X'_{rv} r'v' + X'_{rr} r'r' + X'_{urr} u'r'r' \quad (25)$$

The values for Eq. (25) are given in Table 4. From the table,  $X'_{rv}$  can be neglected due to the large uncertainty. The values of  $X'_{rr}$  and  $X'_{urr}$  are nearly the same. So, it is possible to just keep one of them. Then, the revised version can be obtained:

$$X' = X'_u \dot{u}' + Y'_v v'r' + Y'_r r'r' + X'_{uuu} u'u'u' + X'_{uvv} u'v'v' + X'_{rvu} r'v'u' + X'_{urr} u'r'r' \quad (26)$$

The number of the parameters of the final surge model are reduced from 12 to 5. However, the new model can still provide a satisfactory prediction of the surge forces. It can reproduce the training set with good accuracy, as presented in Fig. 6. The  $R^2$  values for both models are 0.854 and 0.849, respectively. So, the final model for surge motion works well and is more stable than the old one.

Table 4. The values of the parameters and their deviations for the whole surge models

Coef.	Old model Eq.(25)		Revised model Eq.(26)	
	Value	Error (%)	Value	Error (%)
$X'_u$	-1.04E-02	0.60	-1.04E-02	0.61
$X'_{uuu}$	-2.36E-04	1.49	-2.67E-04	1.29
$X'_{uvv}$	-1.34E-02	1.54	-9.29E-03	1.76
$X'_{rvu}$	6.99E-02	4.89	5.84E-02	0.25
$X'_{rv}$	-1.09E-02	29.68	-	-
$X'_{rr}$	6.19E-02	3.13	-	-
$X'_{urr}$	-6.34E-02	3.07	-1.22E-03	2.33



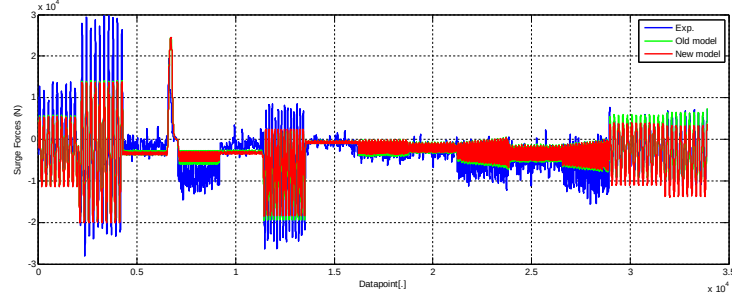


Figure 6: The training set reproduced on the basis of the obtained surge models (Eq. 25 and Eq.26).

## 5.2 Regression analysis of sway motion

First, pure sway test is used as the training set. Because the yaw rate is kept as zero, so the sway model in Eq.(20) can be simplified as:

$$Y' = Y'_{\dot{v}} \dot{v}' + Y'_{uv} u'v' + Y'_{uuv} u'u'v' + Y'_{vvv} v'v'v' + Y'_{|v|} v'|v'| \quad (27)$$

The values of the parameters and deviations are presented in Table 5. The ones with a large uncertainty are neglected and delete similar terms. The Eq.(27) can be rewritten as:

$$Y' = Y'_{\dot{v}} \dot{v}' + Y'_{uuv} u'u'v' + Y'_{|v|} v'|v'| \quad (28)$$

The uncertainty of the parameters diminishes significantly, meanwhile, and the  $R^2$  for both models is 0.9959 and 0.9957, respectively. Obviously, the accuracy of the simplified model is not destroyed, but the parameters obtained are more stable. The pure sway forces are reproduced using the obtained model and it agrees very well with the experiment results, as presented in Fig. 7.

Table 5. The values of the parameters and their deviations for the sway models using pure sway test data.

Coef.	Old model Eq.(27)	Revised model Eq.(28)
-------	-------------------	-----------------------

	Value	Error (%)	Value	Error (%)
$Y'_v$	-3.84E-02	0.13	-3.84E-02	0.14
$Y'_{uv}$	5.05E-01	11.95	-	-
$Y'_{uuv}$	-5.71E-01	10.48	-6.70E-02	0.54
$Y'_{vvv}$	-1.14E-01	10.15	-	-
$Y'_{v v }$	-1.65E-01	5.82	-1.38E-01	1.65

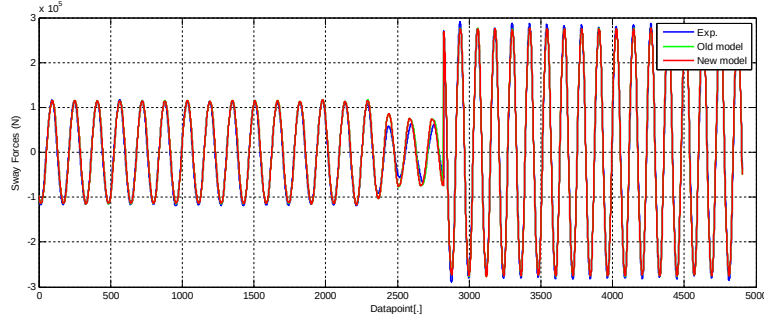


Figure 7: The pure sway test reproduced on the basis of the obtained sway models.

For pure yaw test, the Eq. (20) can be rewritten as:

$$Y' = Y'_r \dot{r}' + X'_u u'r' + Y'_{ur} u'r' + Y'_{uur} u'u'r' + Y'_{urr} r'r'r' + Y'_{r|r|} r'|r'| \quad (29)$$

A simplified model is directly proposed considering the above discussion.

$$Y' = Y'_r \dot{r}' + X'_u u'r' + Y'_{uur} u'u'r' + Y'_{r|r|} r'|r'| \quad (30)$$

The parameters for both models are obtained using the system identification, and the deviations are also given in Table 6.  $R^2$  values for both models are 0.9965 and 0.9962. Fig. 8 shows the sway forces reproduced using the obtained sway model. The numerical prediction agrees very well with the experimental results.

Table 6. The values of the parameters and their deviations for the sway models using pure yaw test data.

Coef.	Old model Eq.(29)		Revised model Eq.(30)	
	Value	Error (%)	Value	Error (%)
$Y'_r$	-1.53E-04	3.41	-1.52E-04	3.56

$Y'_{ur}$	2.75E+00	57.32	-	-
$Y'_{uur}$	-2.72E+00	57.90	3.00E-02	0.14
$Y'_{rrr}$	-6.87E-03	2.64	-	-
$Y'_{r r }$	1.16E-02	2.09	2.70E-03	2.36

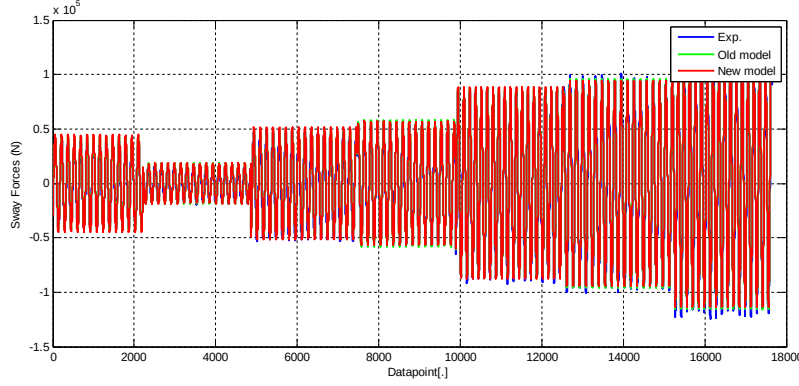


Figure 8: The pure yaw test reproduced on the basis of the obtained sway models.

Finally, the sway models in Eq. (20) can be expressed as in Eq. (31) when similar terms have been deleted.

$$Y' = X'_{\dot{u}} u'r' + Y'_{\dot{v}} \dot{v}' + Y'_{uv} u'u'v' + Y'_{v|v|} v'|v'| + Y'_{\dot{r}} \dot{r}' + Y'_{uur} u'u'r' + Y'_{r|r|} r'|r'| + Y'_{v|r|} v'|r'| + Y'_{r|v|} r'|v'| \quad (31)$$

With this model, the estimated parameters and deviations are presented in Table 7. From the table, the parameters,  $Y'_{r|r|}$  and  $Y'_{v|v|}$ , can be neglected. So, the new model can be written as:

$$Y' = X'_{\dot{u}} u'r' + Y'_{\dot{v}} \dot{v}' + Y'_{uv} u'u'v' + Y'_{v|v|} v'|v'| + Y'_{\dot{r}} \dot{r}' + Y'_{uur} u'u'r' + Y'_{r|v|} r'|v'| \quad (32)$$

The  $R^2$  values for both models are 0.9913 and 0.9912, respectively. So, the new model can predict the sway forces with good accuracy. The sway forces reproduced using the obtained numerical models are presented in Fig. 9.

Table 7. The values of the parameters and their deviations for the sway models using mixed PMM tests.

Coef.	Old model Eq.(31)	New model Eq.(32)
-------	-------------------	-------------------

	Value	Error (%)	Value	Error (%)
$Y'_v$	-3.82E-02	0.14	-3.82E-02	0.14
$Y'_{uvv}$	-6.22E-02	0.18	-6.16E-02	0.18
$Y'_{v v }$	-1.23E-01	0.28	-1.22E-01	0.28
$Y'_r$	-2.68E-04	3.81	-2.66E-04	3.85
$Y'_{uur}$	3.07E-02	0.25	3.13E-02	0.09
$Y'_{r r }$	1.04E-03	10.66	-	-
$Y'_{v r }$	2.01E-04	5.95	-	-
$Y'_{r v }$	1.14E-03	0.91	1.12E-03	0.91

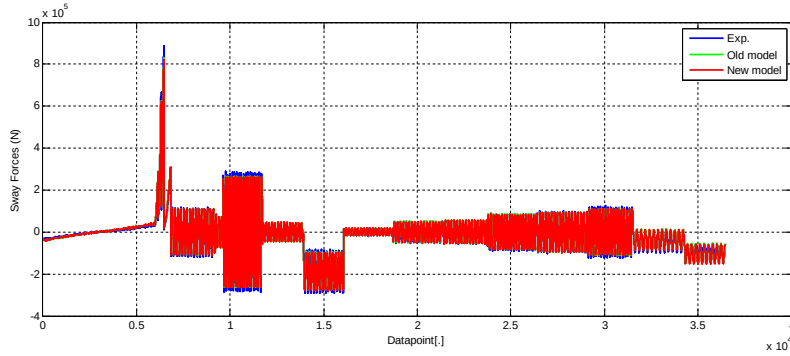


Figure 9: The sway forces of mixed PMM test reproduced using the obtained sway models.

### 5.3 Regression analysis of yaw motion

First, pure yaw tests are used as the training test, and the yaw model can be simplified considering the zero-sway velocity. With the above discussion, the term,  $N'_{rrr}$ , is deleted due to its similar effect with the parameter  $N'_{r|r|}$ . A new yaw model can be written as

$$N' = N'_r \dot{r}' + Y'_r u'r' + N'_{ur} u'r' + N'_{uur} u'u'r' + N'_{r|r|} r'|r'| \quad (33)$$

The values and deviations are presented in Table 8. Obviously,  $N'_{ur}$  and  $N'_{uur}$  fail to be estimated. So, it is a necessity to delete one of them. A new model can be given:

$$N' = N'_r \dot{r}' + Y'_r u'r' + N'_{uur} u'u'r' + N'_{r|r|} r'|r'| \quad (34)$$

The values of the new model are presented in Table 8. The parameters are more stable and the  $R^2$  value of both models are almost same, ( $R^2 = 0.9972$ ). Both models are used to reproduce the sway moment during the pure sway test. The results are presented in Fig. 10.

Table 8. The values of the parameters and their deviations for the yaw models using pure yaw test data.

Coef.	Old model Eq.(33)		New model Eq.(34)	
	Value	Error (%)	Value	Error (%)
$N'_r$	-1.25E-03	0.11	-1.25E-03	0.11
$N'_{ur}$	2.48E+00	17.21	-	-
$N'_{uur}$	-2.48E+00	17.15	-7.62E-03	0.15
$N'_{r v }$	-2.23E-03	0.74	-2.23E-03	0.74

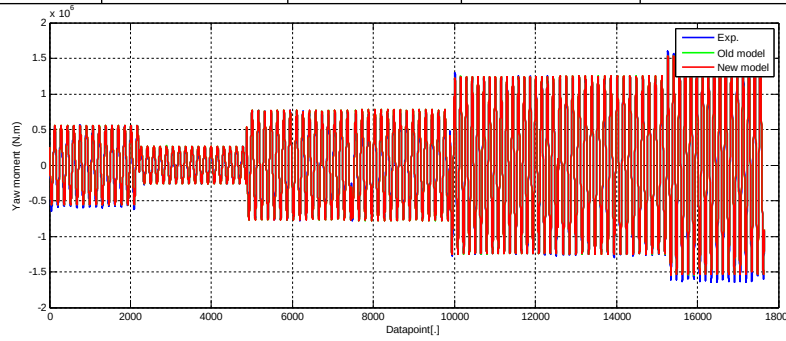


Figure 10: The pure yaw test reproduced on the basis of the obtained yaw models.

Then, the pure sway test will be used to estimate the parameters of the yaw model.

Considering the similar terms, the yaw model can be rewritten as:

$$N' = N'_\dot{v} \dot{v}' + (Y'_v - X'_u) v' u' + N'_{uv} u' v' + N'_{uuv} u' u' v' + N'_{v|v|} v' |v'| \quad (35)$$

The parameters in Eq. (35) can be estimated and the corresponded deviations are presented in Table 9. From the table, the terms  $N'_{uv}$  and  $N'_{v|v|}$  are deleted due to the large uncertainty. So, a revised version is:

$$N' = N'_\dot{v} \dot{v}' + (Y'_v - X'_u) v' u' + N'_{uuv} u' u' v' \quad (36)$$

The parameters of the new model are also presented in Table 9. The  $R^2$  values of both models are 0.964 and 0.962, respectively.

Table 9. The values of the parameters and their deviation for the yaw models using pure yaw test data.

Coef.	Old model Eq.(35)		New model Eq.(36)	
	Value	Error (%)	Value	Error (%)
$N'_\psi$	1.92E-03	0.55	1.92E-03	0.56
$N'_{uv}$	-9.10E-02	13.23	-	-
$N'_{uuv}$	8.40E-02	14.24	-7.23E-03	0.33
$N'_{v r }$	5.91E-03	26.79	-	-

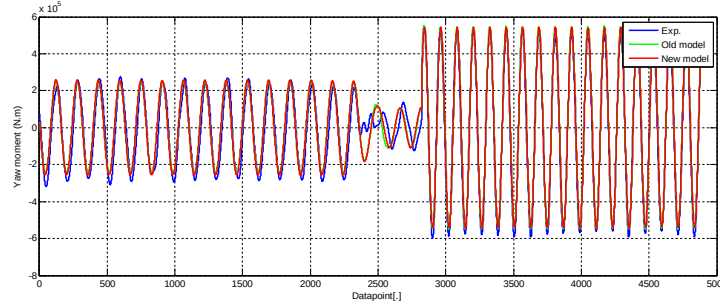


Figure 11: The yaw moment of pure sway test reproduced using the obtained yaw models.

The sway moment reproduced using the numerical models agrees very well with the experimental results, as shown in Fig. 11.

With the previous discussion, Eq. (21) can be rewritten as:

$$\begin{aligned}
 N' = & Y'_r u'r' + (Y'_v - X'_u)v'u' + N'_r \dot{r}' + N'_{uv}u'u'r' + N'_{r|r}|r'| \\
 & + N'_v \dot{v}' + N'_{uuv}u'u'v' + N'_{vrv}v'r'r' + N'_{rvv}r'v'v' + N'_{v|r}|r'| + N'_{r|v}|v'|
 \end{aligned} \quad (37)$$

Obviously, there are similar terms in Eq. (37). So, a modified version can be proposed as:

$$N' = Y'_r u'r' + (Y'_v - X'_u)v'u' + N'_r \dot{r}' + N'_{uv}u'u'r' + N'_{r|r}|r'| + N'_v \dot{v}' + N'_{uuv}u'u'v' + N'_{v|r}|r'| + N'_{r|v}|v'|$$

(38)

The values of the parameters and the deviations of both yaw models are presented in Table 10. The parameters,  $N'_{vrr}$  and  $N'_{rvv}$ , are the ones with a larger uncertainty. So, it is necessary to delete them in the modified version. The  $R^2$  value of both models are 0.9941 and 0.9937, respectively, but the parameters of the new model are more robust. The obtained numerical yaw model is used to predict the yaw moment during the mixed PMM tests, as presented in Fig. 12. The numerical predictions are in good agreement with the experimental results.

Table 10. The values of the parameters and their deviation for the yaw models using pure yaw test data.

Coef.	Old model Eq.(37)		New model Eq.(38)	
	Value	Error (%)	Value	Error (%)
$N'_r$	-1.20E-03	0.19	-1.20E-03	0.19
$N'_{uur}$	-8.21E-03	0.21	-8.41E-03	0.20
$N'_{r v }$	-1.24E-03	2.03	-1.00E-03	2.50
$N'_v$	1.88E-03	0.63	1.87E-03	0.65
$N'_{uuv}$	2.13E-02	0.11	2.14E-02	0.10
$N'_{vrr}$	6.05E-01	2.64	-	-
$N'_{rvv}$	-2.86E-03	9.63	-	-
$N'_{v r }$	-2.35E-02	0.79	-1.69E-02	0.40
$N'_{r v }$	1.28E-02	1.42	1.11E-02	0.73

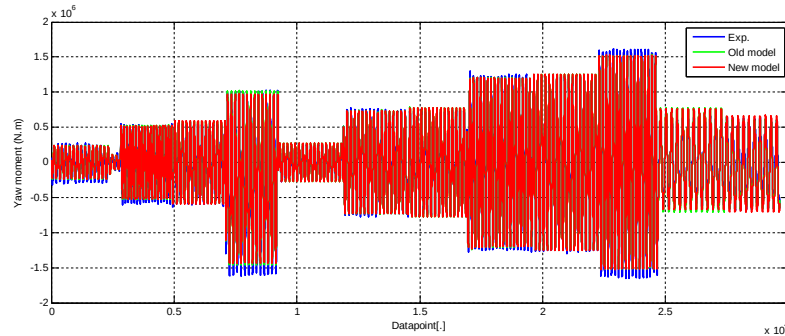


Figure. 12 The yaw moment in the mixed PMM tests reproduced using the obtained yaw models.

## 6. Validation of the simplified nonlinear manoeuvring model

In this section, the final version of the nonlinear manoeuvring model is summarized, and nondimensional hydrodynamic coefficients are also presented. In order to validate the obtained numerical model, all of the PMM test data are used as the test data. The training data, which was used in the proceeding section, takes only a small portion. With the discussion in the preceding section, the final equations of the hydrodynamic forces and moment can be expressed as follow:

$$X' = X'_u \dot{u}' + Y'_v \dot{v}' + Y'_r r' + X'_{uuu} u' u' u' + X'_{uvv} u' v' v' + X'_{rvu} r' v' u' + X'_{urr} u' r' r' \quad (39)$$

$$Y' = X'_u u' r' + Y'_v \dot{v}' + Y'_{uvv} u' u' v' + Y'_{v|v} v' |v'| + Y'_r \dot{r}' + Y'_{urr} u' u' r' + Y'_{r|v} r' |v'| \quad (40)$$

$$N' = Y'_r u' r' + (Y'_v - X'_u) v' u' + N'_r \dot{r}' + N'_{urr} u' u' r' + N'_{r|r} r' |r'| + N'_v \dot{v}' + N'_{uvv} u' u' v' + N'_{v|v} v' |v'| + N'_{r|v} r' |v'| \quad (41)$$

Or rewrite the nonlinear damping matrix as:

$$D(\mathbf{v}) = \begin{bmatrix} -X'_{uuu} u^2 - X'_{uvv} v r & -X'_{uvv} u v & -X'_{urr} u r \\ 0 & -Y'_{uvv} u^2 - Y'_{v|v} |v| & -Y'_{urr} u^2 - Y'_{v|r} |v| \\ 0 & -N'_{uvv} u^2 - N'_{r|v} |r| & -N'_{urr} u^2 - N'_{v|r} |v| - N'_{r|r} |r| \end{bmatrix} \quad (42)$$

The final version of the nonlinear manoeuvring model is more simplified compared with the previous ones, which are described in Eq. (19-21). There are 18 hydrodynamic coefficients in the surge, sway and yaw model, but 38 for the previous models. Then the truncated LS-SVM was used to estimate the values of the hydrodynamic coefficients of the simplified models. The nondimensional hydrodynamic coefficients are presented in Table



11. The obtained parameters are stable and with a smaller deviation. The revised version is much simpler compared with the models in Eq. (19-21), but it can also provide a very good prediction of the surge, sway forces and yaw moment.

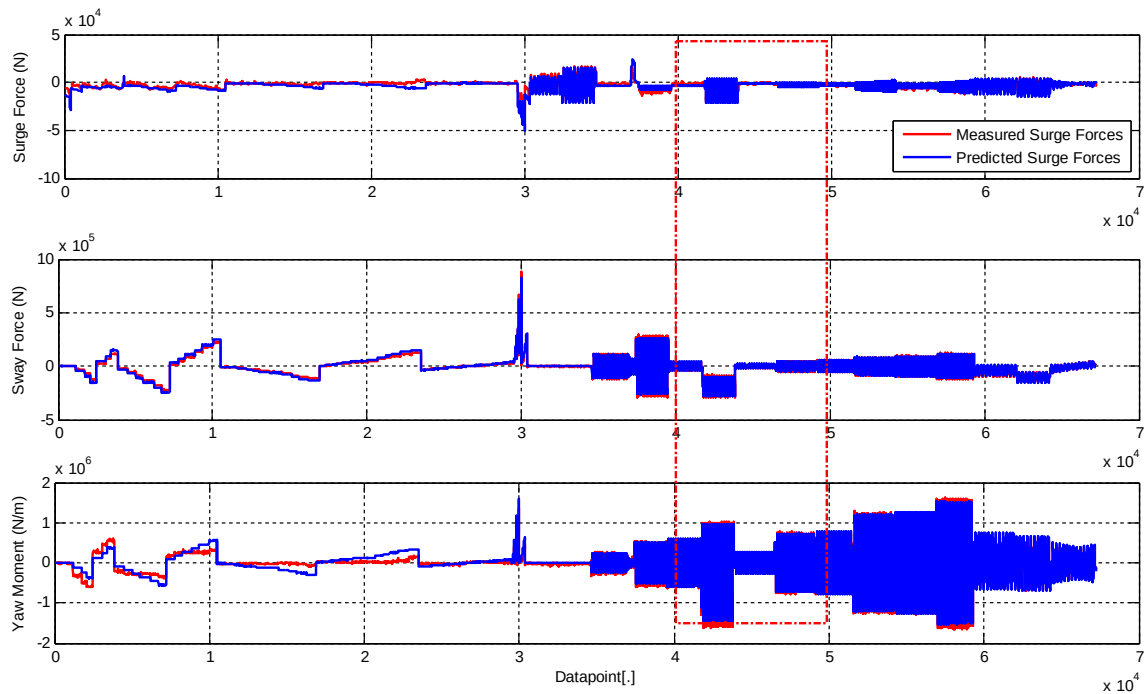
As presented in Table 12, the  $R^2$  values indicate that the obtained numerical models reproduced the experimental results successfully. It is also confirmed in Fig. 13. The prediction of the surge, sway force and yaw moment are in very good agreement with the experimental results. From Table 11, the obtained parameters using the truncated LS-SVM are very stable and the deviations are very small. The small deviations indicate that the obtained values are very near the true values. Parameter drift or uncertainty is diminished successfully. As discussed in the previous section, the identified parameters are stable with the noise. Meanwhile, the obtained manoeuvring model can predict the hydrodynamic forces and moment accurately, as presented in Table 12. So, the simplified manoeuvring model can be used to describe the motion of ship.

Table 11. The values of the parameters and their deviations of the nonlinear simplified manoeuvring models

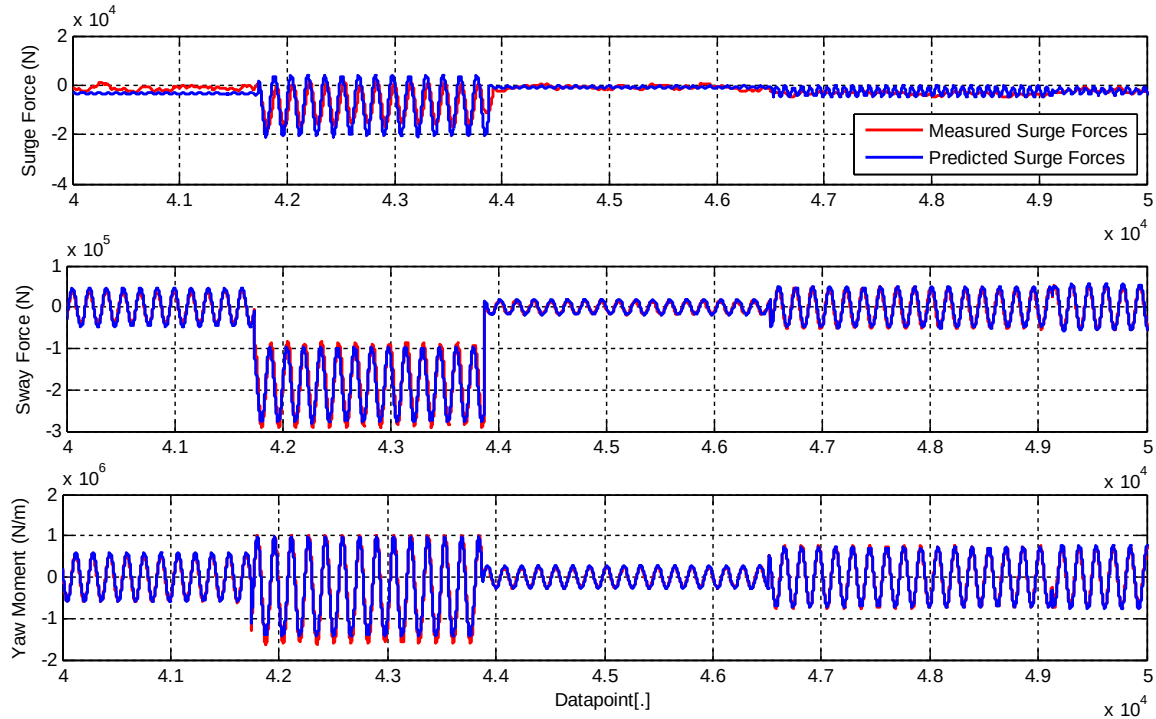
Coef.	Value	Error (%)	Coef.	Value	Error (%)	Coef.	Value	Error (%)
$X'_{\dot{u}}$	-1.04E-02	0.61	$Y'_v$	-3.82E-02	0.14	$N'_r$	-1.20E-03	0.19
$X'_{uuu}$	-2.67E-04	1.29	$Y'_r$	-2.66E-04	3.85	$N'_v$	1.87E-03	0.65
$X'_{uvv}$	-9.29E-03	1.76	$Y'_{uvv}$	-6.16E-02	0.18	$N'_{uur}$	-8.41E-03	0.20
$X'_{rvu}$	5.84E-02	0.25	$Y'_{v v }$	-1.22E-01	0.28	$N'_{r v }$	-1.00E-03	2.50
$X'_{urr}$	-1.22E-03	2.33	$Y'_{uur}$	3.13E-02	0.09	$N'_{uvv}$	2.14E-02	0.10
			$Y'_{r v }$	1.12E-03	0.91	$N'_{v v }$	-1.69E-02	0.40
						$N'_{r v }$	1.11E-02	0.73

Table 12. The  $R^2$  goodness of fit criterion for validation.

	Surge	Sway	Yaw
$R^2$	0.6862	0.9811	0.9501



(a)



(b)

Figure 13: The surge and sway forces and yaw moment reproduced using the revised version of the nonlinear manoeuvring model (a). (b) is a partial enlargement view at red rectangular region.

## Conclusions

This paper proposed a novel version of least square support vector machine, the truncated least square support vector machine (LS-SVM), and used it to estimate the hydrodynamic coefficients of a nonlinear manoeuvring model of a ship. Singular value decomposition was used to analyse the parameter drift, which can be ascribed to the ill-conditioned kernel matrix. Truncated LS-SVM was implemented with the optimal truncated singular values decomposition of the kernel matrix, which neglected the small singular values and the corresponding matrix. Meanwhile, this operation also reduces the dimensionality of the kernel matrix, which increases the computation efficiency.

A nonlinear manoeuvring mathematical model of a surface ship in 3-DOF was derived and the hydrodynamic coefficients have been converted to the dimensionless ones using the

prime system of SNAME [43]. The structure of nonlinear manoeuvring model is too complex, and it almost certainly results in overfitting and multicollinearity. In order to diminish the multicollinearity and obtained a robust parameter estimation, the truncated LS-SVM and the leave-one-out method was used for model reduction offline. The results show that the simplified manoeuvring models are still with the same accuracy.

The parameters of the revised numerical model were estimated using truncated LS-SVM. The obtained parameters are very stable and with the absolute errors are very small, which indicated the parameter drift is diminished successfully. The PMM test data was used to validate the obtained numerical model. The results agree very well with the experimental results, which indicated the resulted manoeuvring model is adequate for modelling the motion of the marine ship.

### **Acknowledgements**

This work was performed within the Strategic Research Plan of the Centre for Marine Technology and Ocean Engineering (CENTEC), which is financed by Portuguese Foundation for Science and Technology (Fundação para a Ciência e Tecnologia-FCT) under contract UID/Multi/00134/2013 - LISBOA-01-0145-FEDER-007629. This work is a contribution to the project M&MSHIPS -“Maneuvering & Moored SHIPS in ports” (PTDC/EMSTRA/5628/2014) funded by the FCT. This work was partly supported by the Research Council of Norway through the Centres of Excellence funding scheme, Project number 223254 - AMOS. The PMM data were collected in the course of the Knowledge-building Project for the Industry "Sea Trials and Model Tests for Validation of Shiphandling Simulation Models", supported by the Research Council of Norway. The first

author is grateful to Prof. Asgeir Sørensen, who is the director of NTNU AMOS, for generous support during the visit in AMOS-NTNU.

## REFERENCES

- [1] J.M. Varela, C. Guedes Soares, Interactive 3D desktop ship simulator for testing and training offloading manoeuvres, *Appl. Ocean Res.* 51 (2015) 367–380.
- [2] J.M. Varela, C. Guedes Soares, Software architecture of an interface for three-dimensional collision handling in maritime Virtual Environments, *Simulation*. 91 (2015) 735–749.
- [3] T.A. Johansen, T.I. Fossen, B. Vik, Hardware-in-the-loop Testing of DP systems, in: *Dyn. Position. Conf.*, Houston, US, 2005: pp. 2–16.
- [4] A.J. Sørensen, A survey of dynamic positioning control systems, *Annu. Rev. Control.* 35 (2011) 123–136.
- [5] F. Dukan, M. Ludvigsen, A.J. Sorensen, Dynamic positioning system for a small size ROV with experimental results, in: *IEEE - Ocean.*, IEEE, Spain, 2011: pp. 1–10.
- [6] M.A. Abkowitz, Measurement of hydrodynamic characteristics from ship maneuvering trials by system identification, *SNAME Trans.* 88 (1980) 283–318.
- [7] K. Nomoto, K. Taguchi, K. Honda, S. Hirano, On the Steering Qualities of Ships, *J. Zosen Kiokai.* 1956 (1956) 75–82.
- [8] Y. Yoshimura, Mathematical model for manoeuvring ship motion (MMG Model), in: *Work. Math. Model. Oper. Involv. Ship-Sh. Interact.*, Kansai Zōsen Kyōkai Kyōkai, 2005: pp. 1–6.
- [9] A. Ogawa, H. Kasai, On the mathematical model of manoeuvring motion of ships,

- Int. Shipbuild. Prog. 25 (1978) 306–319.
- [10] T.I. Fossen, Handbook of Marine Craft Hydrodynamics and Motion Control, John Wiley & Sons, Ltd, Chichester, UK, 2011.
- [11] S. Sutulo, C. Guedes Soares, Mathematical models for simulation of manoeuvring performance of ships, in: C. Guedes Soares, Y. Garbatov, N. Fonseca, A.P. Teixeira (Eds.), Marit. Eng. Technol., Taylor & Francis Group, London, 2011: pp. 661–698.
- [12] S. Sutulo, C. Guedes Soares, Development of a core mathematical model for arbitrary manoeuvres of a shuttle tanker, Appl. Ocean Res. 51 (2015) 293–308.
- [13] Y. Yoshimura, H. Sakurai, Mathematical Model for the Manoeuvring Ship Motion in Shallow Water (3rd Report) : Manoeuvrability of a Twin-propeller Twin rudder ship, J. Kansai Soc. Nav. Archit. Japan. (1989).
- [14] M. Vantorre, K. Eloit, G. Delefortrie, E. Lataire, M. Candries, J. Verwilligen, Maneuvering in Shallow and Confined Water, in: Encycl. Marit. Offshore Eng., John Wiley & Sons, Ltd, Chichester, UK, 2017: pp. 1–17.
- [15] G. Delefortrie, M. Tello Ruiz, M. Vantorre, Manoeuvring model of an estuary container vessel with two interacting Z-drives, J. Mar. Sci. Technol. (2017) 1–15.
- [16] G. Delefortrie, K. Eloit, E. Lataire, W. Van Hoydonck, M. Vantorre, Captive model tests based 6 DOF shallow water manoeuvring model, in: Proc. 4th MASHCON, 2016.
- [17] L. Ljung, System identification : theory for the user, Prentice Hall PTR, 1999.
- [18] ITTC, Manoeuvrability Captive Model Test Procedure, in: 23rd Int. Towing Tank Conf., 2002.
- [19] B. Golding, A. Ross, T.I. Fossen, Identification of nonlinear viscous damping for

- marine vessels, in: 14 Th IFAC Symp. Syst. Identif., Newcastle , Australia , 2006, 2006: pp. 332–337.
- [20] S. Sutulo, C. Guedes Soares, An algorithm for offline identification of ship manoeuvring mathematical models from free-running tests, *Ocean Eng.* 79 (2014) 10–25.
- [21] W.L. Luo, Z.J. Zou, Parametric Identification of Ship Maneuvering Models by Using Support Vector Machines, *J. Sh. Res.* 53 (2009) 19–30.
- [22] W. Luo, C. Guedes Soares, Z. Zou, Parameter Identification of Ship Maneuvering Model Based on Support Vector Machines and Particle Swarm Optimization, *J. Offshore Mech. Arct. Eng.* 138 (2016) 031101.
- [23] H.T. Xu, M.A. Hinostroza, C. Guedes Soares, Estimation of Hydrodynamic Coefficients of a Nonlinear Manoeuvring Mathematical Model with Free-Running Ship Model Tests, *Int. J. Marit. Eng.* 160 (2018) A-213-A-226.
- [24] K.J. Åström, C.G. Källström, Identification of ship steering dynamics, *Automatica.* 12 (1976) 9–22.
- [25] A. Ross, O. Selvik, V. Hassani, E. Ringen, D. Fathi, Identification of Nonlinear Manoeuvring Models for Marine Vessels using Planar Motion Mechanism Tests, in: ASME 2015 34th Int. Conf. Ocean. Offshore Arct. Eng., ASME, Newfoundland, Canada, 2015: p. V007T06A014.
- [26] P.W.J. van de Ven, T.A. Johansen, A.J. Sørensen, C. Flanagan, D. Toal, Neural network augmented identification of underwater vehicle models, *Control Eng. Pract.* 15 (2007) 715–725.
- [27] V. Hassani, D. Fathi, A. Ross, F. Sprenger, Ø. Selvik, T.E.T.E. Berg, D. Fathi, F.

- Sprenger, T.E.T.E. Berg, Time domain simulation model for research vessel Gunnerus, in: ASME 2015 34th Int. Conf. Ocean. Offshore Arct. Eng., ASME, Newfoundland, Canada, 2015: p. V007T06A013.
- [28] S. Sutulo, C. Guedes Soares, Offline System Identification of Ship Manoeuvring Mathematical Models with a Global Optimization Algorithm, in: MARSIM 2015, Newcastle, United Kingdom, 2015: pp. 28–43.
- [29] M.A. Hinostroza, H.T. Xu, C. Guedes Soares, Experimental and numerical simulations of zig-zag manoeuvres of a self-running ship model, in: C. Guedes Soares, T. A.P. (Eds.), Marit. Transp. Harvest. Sea Resour., Taylor & Francis Group, London, UK, 2017: pp. 563–570.
- [30] T. Söderström, Comparing some classes of bias-compensating least squares methods, *Automatica*. 49 (2013) 840–845.
- [31] G.H. Golub, C. Reinsch, Singular value decomposition and least squares solutions, *Numer. Math.* 14 (1970) 403–420.
- [32] T.F. Chan, P.C. Hansen, Computing Truncated Singular Value Decomposition Least Squares Solutions by Rank Revealing QR-Factorizations, *SIAM J. Sci. Stat. Comput.* 11 (1990) 519–530.
- [33] P. Hansen, Rank-deficient and discrete ill-posed problems: numerical aspects of linear inversion, *Soc. Ind. Appl. Math.* (1998) 175–208.
- [34] J.B. Bell, A.N. Tikhonov, V.Y. Arsenin, Solutions of Ill-Posed Problems., *Math. Comput.* 32 (1978) 1320–1322.
- [35] G.H. Golub, P.C. Hansen, D.P. O’Leary, Tikhonov Regularization and Total Least Squares, *SIAM J. Matrix Anal. Appl.* 21 (1999) 185–194.



- [36] P.C. Hansen, D.P. O’Leary, The Use of the L-Curve in the Regularization of Discrete Ill-Posed Problems, *SIAM J. Sci. Comput.* 14 (1993) 1487–1503.
- [37] D. Ma, W. Tan, Z. Zhang, J. Hu, Parameter identification for continuous point emission source based on Tikhonov regularization method coupled with particle swarm optimization algorithm, *J. Hazard. Mater.* 325 (2017) 239–250.
- [38] L.P. Perera, P. Oliveira, C. Guedes Soares, System Identification of Nonlinear Vessel Steering, *J. Offshore Mech. Arct. Eng.* 137 (2015) 031302.
- [39] L.P. Perera, P. Oliveira, C. Guedes Soares, System identification of vessel steering with unstructured uncertainties by persistent excitation maneuvers, *IEEE J. Ocean. Eng.* 41 (2016) 515–528.
- [40] A. Tiano, R. Sutton, A. Lozowicki, W. Naeem, Observer Kalman filter identification of an autonomous underwater vehicle, *Control Eng. Pract.* 15 (2007) 727–739.
- [41] V. Hassani, A.J. Sørensen, A.M. Pascoal, Adaptive wave filtering for dynamic positioning of marine vessels using maximum likelihood identification: Theory and experiments, in: *IFAC Proc. Vol.*, 2013: pp. 203–208.
- [42] C. Cortes, V. Vapnik, Support-Vector Networks, *Mach. Learn.* 20 (1995) 273–297.
- [43] J.A.K. Suykens, J. Vandewalle, Least Squares Support Vector Machine Classifiers, *Neural Process. Lett.* 9 (1999) 293–300.
- [44] V.N. Vapnik, *The Nature of Statistical Learning Theory*, Springer. 8 (1995) 187.
- [45] T. Falck, P. Dreesen, K. De Brabanter, K. Pelckmans, B. De Moor, J.A.K. Suykens, Least-Squares Support Vector Machines for the identification of Wiener–Hammerstein systems, *Control Eng. Pract.* 20 (2012) 1165–1174.
- [46] X.-C. Xi, A.-N. Poo, S.-K. Chou, Support vector regression model predictive control

- on a HVAC plant, *Control Eng. Pract.* 15 (2007) 897–908.
- [47] H.T. Xu, C. Guedes Soares, Vector field path following for surface marine vessel and parameter identification based on LS-SVM, *Ocean Eng.* 113 (2016) 151–161.
- [48] H.T. Xu, M.A. Hinostroza, V. Hassani, C. Guedes Soares, Real-Time Parameter Estimation of a Nonlinear Vessel Steering Model Using a Support Vector Machine, *J. Offshore Mech. Arct. Eng.* 141 (2019) 061606.
- [49] H.T. Xu, C. Guedes Soares, Waypoint-following for a marine surface ship model based on vector field guidance law, in: C. Guedes Soares, T.A. Santos (Eds.), *Marit. Technol. Eng.* 3, Taylor & Francis Group, London, UK, 2016: pp. 409–418.
- [50] H. Xu, V. Hassani, C. Guedes Soares, Uncertainty analysis of the hydrodynamic coefficients estimation of a nonlinear manoeuvring model based on planar motion mechanism tests, *Ocean Eng.* 173 (2019) 450–459.
- [51] H.T. Xu, C. Guedes Soares, An optimized energy-efficient path following algorithm for underactuated marine surface ship model, *Int. J. Marit. Eng.* 160 (2018) A-411-A-421.
- [52] W. Luo, L. Moreira, C. Guedes Soares, Manoeuvring simulation of catamaran by using implicit models based on support vector machines, *Ocean Eng.* 82 (2014) 150–159.
- [53] X.-R. Hou, Z.-J. Zou, Parameter identification of nonlinear roll motion equation for floating structures in irregular waves, *Appl. Ocean Res.* 55 (2016) 66–75.
- [54] W. Luo, X. Li, Measures to diminish the parameter drift in the modeling of ship manoeuvring using system identification, *Appl. Ocean Res.* 67 (2017) 9–20.
- [55] W. Hwang, *Application of System Identification to Ship Maneuvering*,

Massachusetts Institute of Technology, 1980.

- [56] H.T. Xu, V. Hassani, C. Guedes Soares, Parameters Estimation of Nonlinear Manoeuvring Model for Marine Surface Ship Based on PMM Tests, in: ASME 2018 37th Int. Conf. Ocean. Offshore Arct. Eng., ASME, Madrid, Spain, 2018: p. V11BT12A010.
- [57] T. Wei, S. Zhongke, L. Hongchao, Denoising of impulse response using LS-SVM and SVD for aircraft flight flutter test, in: Syst. Control Aerosp. Astronaut. 2006. ISSCAA 2006. 1st Int. Symp., IEEE, 2006: pp. 684. – 688.
- [58] P.-P. Zheng, J. Feng, Z. Li, M. Zhou, A novel SVD and LS-SVM combination algorithm for blind watermarking, *Neurocomputing*. 142 (2014) 520–528.
- [59] J.A.K. Suykens, T. Van Gestel, J. De Brabanter, B. De Moor, J. Vandewalle, *Least Squares Support Vector Machines*, 2002.
- [60] P.C. Hansen, P.R. Johnston, The L-Curve and its Use in the Numerical Treatment of Inverse Problems, in: *Comput. Inverse Probl. Electrocardiogr.*, 2001: pp. 119–142.
- [61] A. Ross, *Nonlinear Manoeuvring Models for Ships: A Lagrangian Approach*, PhD Thesis, Norwegian University of Science and Technology, 2008.
- [62] H. Korte, J.-H. Wesuls, S. Stuppe, T. Takagi, Towards an Approach to 6 DOF Inertial Kinematics, *IFAC-PapersOnLine*. 49 (2016) 440–445.
- [63] A. Ross, T. Perez, T.I. Fossen, A novel manoeuvring model based on low-aspect-ratio lift theory and lagrangian mechanics, *IFAC Proc. Vol. 40* (2007) 229–234.
- [64] SNAME, *Nomenclature for treating the motion of a submerged body through a fluid*, Society of Naval Architects and Marine Engineers, New York, 1950.